

编号: 2025-1233

## 检索报告

受南通市第一人民医院王耀的委托,对其所提交的学术论文被收录和引用情况在 Web of Science(Science Citation Index Expanded)中进行了检索,以下 1 篇论文被 SCIE 收录。

第 1 条,共 1 条

**标题: miR-210 Regulates Autophagy Through the AMPK/mTOR Signaling Pathway, Reduces Neuronal Cell Death and Inflammatory Responses, and Enhances Functional Recovery Following Cerebral Hemorrhage in Mice**

作者: Wang, Y (Wang, Yao); Jiang, L (Jiang, Lei); Tian, JJ (Tian, Jin-jie); Zhu, LL (Zhu, Lin-lin); Dai, HJ (Dai, He-jun); Guo, C (Guo, Chao); Zhou, LY (Zhou, Ling-yun); Wang, L (Wang, Lei); Lu, Y (Lu, Yong); Zhang, Y (Zhang, Yi)

来源出版物: NEUROCHEMICAL RESEARCH 卷: 50 期: 3 文献号: 180

DOI: 10.1007/s11064-025-04434-7 Published Date: 2025 JUN

Web of Science 核心合集中的 "被引频次": 0

入藏号: WOS:001503932600004

文献类型: Article

地址: [Wang, Yao; Jiang, Lei; Tian, Jin-jie; Guo, Chao; Zhang, Yi] Nantong Univ, Dept Neurosurg, Affiliated Hosp 2, Nantong, Jiangsu, Peoples R China.

[Zhu, Lin-lin; Lu, Yong] Nantong Univ, Dept Nursing, Affiliated Hosp 2, Nantong, Jiangsu, Peoples R China.

[Dai, He-jun] Nantong Univ, Affiliated Danyang Hosp, Dept Neurosurg, Jiangsu, Peoples R China.

[Zhou, Ling-yun] Heilongjiang Univ Chinese Med, Affiliated Hosp 1, Dept Acupuncture & Moxibust, Harbin, Peoples R China.

[Wang, Lei] Nantong Univ, Affiliated Hosp 2, Dept Emergency, Nantong, Jiangsu, Peoples R China.

通讯作者地址: Zhang, Y (通讯作者), Nantong Univ, Dept Neurosurg, Affiliated Hosp 2, Nantong, Jiangsu, Peoples R China.

Lu, Y (通讯作者), Nantong Univ, Dept Nursing, Affiliated Hosp 2, Nantong, Jiangsu, Peoples R China.

Wang, L (通讯作者), Nantong Univ, Affiliated Hosp 2, Dept Emergency, Nantong, Jiangsu, Peoples R China.

电子邮件地址: wangleilei2339@163.com; luyong11274522@163.com; zhangyi9285@sina.com

ISSN: 0364-3190

eISSN: 1573-6903

期刊影响因子 (2024): 3.8

中科院 2025 年期刊大类分区 (升级版): 3 区

特此证明!





# miR-210 Regulates Autophagy Through the AMPK/mTOR Signaling Pathway, Reduces Neuronal Cell Death and Inflammatory Responses, and Enhances Functional Recovery Following Cerebral Hemorrhage in Mice

Yao Wang<sup>1</sup> · Lei Jiang<sup>1</sup> · Jin-jie Tian<sup>1</sup> · Lin-lin Zhu<sup>2</sup> · He-jun Dai<sup>3</sup> · Chao Guo<sup>1</sup> · Ling-yun Zhou<sup>4</sup> · Lei Wang<sup>5</sup> · Yong Lu<sup>2</sup> · Yi Zhang<sup>1</sup>

Received: 8 January 2025 / Revised: 14 April 2025 / Accepted: 20 May 2025  
© The Author(s) 2025

## Abstract

Recently, a growing body of research has shown that microRNAs (miRNAs) are crucial in the pathophysiological mechanisms of brain disorders, *miR-210* is one of the significant miRNAs implicated in these disorders, and its function in intracerebral hemorrhage (ICH) is not yet fully understood. Research the impact of *miR-210* on intracerebral hemorrhage and probe into its working mechanism. The ICH model was established by injecting collagenase into the basal ganglia of male C57/BL6 mice ( $n=142$ ). Firstly, the mice were divided into sham group ( $n=6$ ) and ICH group ( $n=30$ ) (3 h, 6 h, 12 h, 24 h, 72 h), the samples of the sham group were collected at 48 h after operation, the brain tissues of the left and right basal ganglia were collected in each group. qPCR was used to detect the level of miR-210 in each group. Then, LV-miR-210 was injected into the lateral ventricle to establish a model of miR-210 overexpression, and NS injection was set as a comparison, which was divided into sham group ( $n=15$ ), ICH group ( $n=15$ ), ICH+NS group ( $n=15$ ), and ICH+LV-miR-210 group ( $n=15$ ). Water maze training was started on the 2 d after surgery. qPCR was used to detect the levels of miR-210, iNOS, IL-1 $\beta$ , IL-6, TNF- $\alpha$ , and IL-10 in each group at 3 d after operation. Western blotting was used to detect the levels of p-AMPK/AMPK, p-mTOR/mTOR, Beclin 1, Bax, Bcl-2, and LC3 II/I in each group. Immunofluorescence was used to detect the expression of lentivirus-mediated miR-210 in mouse brain. Water maze was used to evaluate the learning and memory function of the mice. The dry-wet method was used to evaluate brain edema, TUNEL was used to detect the apoptosis of brain cells in each group. Then, Rapamycin and AICAR were used to intervene p-AMPK/AMPK and p-mTOR/mTOR, and they were divided into sham group ( $n=6$ ), ICH group ( $n=6$ ), ICH+LV-miR-210 group ( $n=6$ ), ICH+LV-miR-210+AICAR group ( $n=6$ ), and ICH+LV-miR-210+Rapamycin group ( $n=6$ ). The levels of miR-210 in each group were detected by qPCR at 3 d after operation, and the levels of p-AMPK/AMPK, p-mTOR/mTOR, Beclin 1, Bax, Bcl-2, and LC3 II/I in each group were detected by WB. Finally, HT22 cells were stimulated with Hemin to construct an in vitro intracerebral hemorrhage model, and the time gradient was set (control group, 3 h, 6 h, 12 h, and 24 h). qPCR was used to detect the expression of miR-210 in each group. Then HT22 cells were transfected with lentivirus, and

Yao Wang, Lei Jiang and Jin-jie Tian contributed equally as first authors.

✉ Lei Wang  
wangleilei2339@163.com

✉ Yong Lu  
luyong11274522@163.com

✉ Yi Zhang  
zhangyi9285@sina.com

<sup>1</sup> Department of Neurosurgery, Affiliated Hospital 2 of Nantong University, Jiangsu, China

<sup>2</sup> Department of Nursing, Affiliated Hospital 2 of Nantong University, Jiangsu, China

<sup>3</sup> Department of Neurosurgery, Affiliated Danyang Hospital of Nantong University, Jiangsu, China

<sup>4</sup> Department of Acupuncture and Moxibustion, The First Affiliated Hospital of Harbin Medical University, Harbin, China

<sup>5</sup> Department of Emergency, Affiliated Hospital 2 of Nantong University, Jiangsu, China

rapamycin and AICAR were used to interfere with p-AMPK/AMPK and p-mTOR/mTOR. Control group, Hemin group, Hemin+LV-miR-210 group, Hemin+LV-miR-210+AICAR group, and Hemin+LV-miR-210+Rapamycin group. qPCR was used to detect the level of miR-210 in each group. The levels of p-AMPK/AMPK, p-mTOR/mTOR, Beclin 1, Bax, Bcl-2, and LC3 II/I in each group were detected by Western blotting. miR-210 is significantly increased in a short time after intracerebral hemorrhage in mice. miR-210 can alleviate secondary injury of ICH by improving neurological deficit and reducing brain edema. In addition, upregulation of miR-210 expression inhibited autophagy and alleviated apoptosis and inflammation. In our study, we found that miR-210 significantly inhibited the activation of AMPK/ mTOR pathway triggered by ICH, and the neuroprotective effect of miR-210 was partially reversed when Rapamycin and AICAR reversed this inhibition. At the mechanistic level, miR-210 exerts its function by regulating AMPK/mTOR signaling pathway, thereby inhibiting autophagy and reducing apoptosis and inflammation. Further studies at the cellular level were basically consistent with the above results. miR-210 is up-regulated after ICH and can play a neuroprotective role by regulating the AMPK/mTOR signaling pathway mediated by autophagy, suggesting that it may become a therapeutic target for reducing nerve injury after ICH.

**Keywords** *miR-210* · Cerebral hemorrhage · Autophagy · Apoptosis · Neuroinflammation

## Introduction

Intracerebral hemorrhage (ICH) is a significant health issue, accounting for approximately 15–20% of stroke incidents and characterized by high fatality and illness rates [1]. Furthermore, the incidence of intracerebral hemorrhage (ICH) demonstrates an age-dependent increase, while the elevated long-term mortality rates observed among younger ICH patients raise significant clinical concerns [2, 3]. And available treatment options are limited; and ICH imposes significant medical, economic, and social burdens. The classification of ICH stages typically encompasses the primary injury stage and the secondary injury stage. A haematoma develops subsequent to the abrupt rupture of a cerebral blood vessel. This event leads to mechanical trauma to surrounding tissues and provokes a rapid escalation in intracranial pressure, which is identified as a primary brain injury [4]. Nevertheless, after ICH, secondary inflammation, mitochondrial dysfunction, oxidative stress, blood–brain barrier (BBB) disruption, and alterations in the immune microenvironment significantly impact neuronal apoptosis and the subsequent process of functional recovery [5, 6]. In the past few years, a considerable amount of investigative research has been focused on exploring the process of secondary damage that follows intracerebral hemorrhage, with the main aim of uncovering novel therapeutic interventions aimed at managing this condition.

MicroRNAs (miRNAs) belong to a class of tiny non-coding RNAs, roughly 22 nucleotides long, that bind to the 3' untranslated region (3' UTR) of certain genes. They either cause mRNA degradation or impede the translation process. Accumulating data suggests that miRNAs are pivotal in the meticulous regulation of immune cell development, differentiation, as well as effector functions [7–9]. *miR-210* is recognized as one of the key molecules involved

in the hypoxic response, and its presence is powerfully triggered by hypoxia within numerous cellular and tissue types [10, 11]. *miR-210* has been extensively studied and demonstrated to modulate a wide array of cellular activities, encompassing immune responses. This regulation has been a focal point of research in the field of molecular biology and genetics [12]. Upon activation of B-cells, *miR-210* is upregulated, inhibiting B-cell reactions to hinder the development of autoantibodies linked to aging. It functions as a controller of harmful Th17 cell development under hypoxic circumstances by adjusting HIF-1 $\alpha$ , a crucial transcription factor involved in Th17 differentiation, through a negative feedback loop [13]. Furthermore, *miR-210* demonstrates the capacity to diminish the proinflammatory response in cartilage cells and within the joints of rats that have undergone lipopolysaccharide (LPS)-induced osteoarthritis (OA). This effect is mediated through the targeting of DR6 and the subsequent suppression of the NF- $\kappa$ B signaling pathway [14, 15]. Hence, *miR-210* seemingly serves as a pivotal molecular brake on inflammatory responses in adults. However, the exact function of *miR-210* in the setting of intracerebral hemorrhage (ICH) remains unclear.

The AMPK and mTOR signaling cascades are crucial for cellular growth, division, and energy processes. Studies have shown that *miR-210* promotes the development of hepatocellular carcinoma (HCC) through its regulation of macrophage self-eating. *miR-210* serves as a pivotal modulator of autophagy in M2 macrophages via its interaction with the PI3K/AKT/mTOR signaling cascade. This subsequently has a considerable influence on the growth and spread of HCC cells [16]. Furthermore, under hypoxic conditions, the upregulation of *miR-210* has been demonstrated to prevent cardiomyocyte apoptosis and autophagy, thereby mitigating the detrimental effects of oxygen deprivation on the heart. This protective mechanism also encompasses the modulation of the AMPK/mTOR signaling pathway [17].

In multiple myeloma (MM), the NBR2/miR-561-5p/DLC1 pathway functions to inhibit glycolysis by stimulating the AMPK/mTOR pathway. This finding reveals the probable function of *miR-210* in modulating metabolic activities [18]. Consequently, *miR-210* exerts a significant influence on a multitude of diseases by modulating the AMPK/mTOR signaling pathway. Further research endeavors may elucidate the precise mechanisms underlying the function of *miR-210* within these signaling cascades, thereby presenting novel therapeutic targets for the associated pathologies.

Remarkably, studies involving human participants have shown that *miR-210* serves as a unique indicator for acute cerebral ischemia and congestive heart failure [19], indicating that the findings of preclinical investigations into *miR-210* have the potential to be translated into clinical applications. Therefore, we postulate that it may also play a role in the subsequent injury following intracerebral hemorrhage (ICH) and holds promise as both a biomarker and a therapeutic focus for ICH.

## Methods and Materials

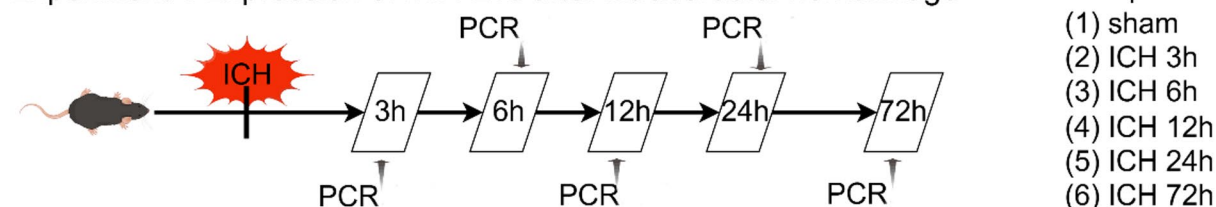
### Animals

The experimental procedures involving 142 male C57/BL6 mice (8 weeks old, weighing between 20 and 25 g) in this study were approved by the Animal Ethics Committee of Nantong University. Mice were randomly assigned to three experimental cohorts (Fig. 1.1), and the allocation of the groups was concealed from the researchers to ensure objectivity. These mice were housed in a controlled environment with optimal conditions of temperature, humidity, and a standardized 12-hour light-dark cycle. Prior to the induction of ICH, the mice were allowed at least three days of acclimation with unrestricted access to food and water.

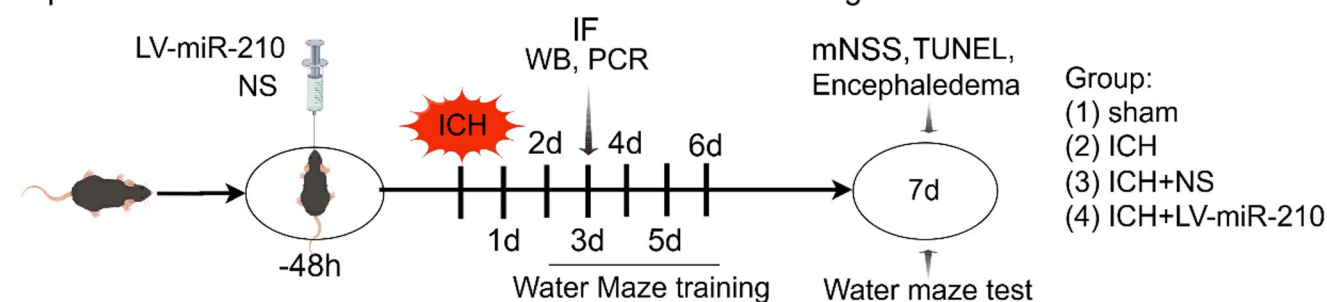
### Establishment of the ICH Model

An ICH mouse model was created through intracranial collagenase injection, following methods outlined in previous literature [4]. The mice were anesthetized with a 2.5% avertin solution (Sigma–Aldrich, St. Louis, MO),

#### Experiment 1 Expression of miR-210 after intracerebral hemorrhage



#### Experiment 2 The role of miR-210 in intracerebral hemorrhage



#### Experiment 3 Mechanism of miR-210 after ICH

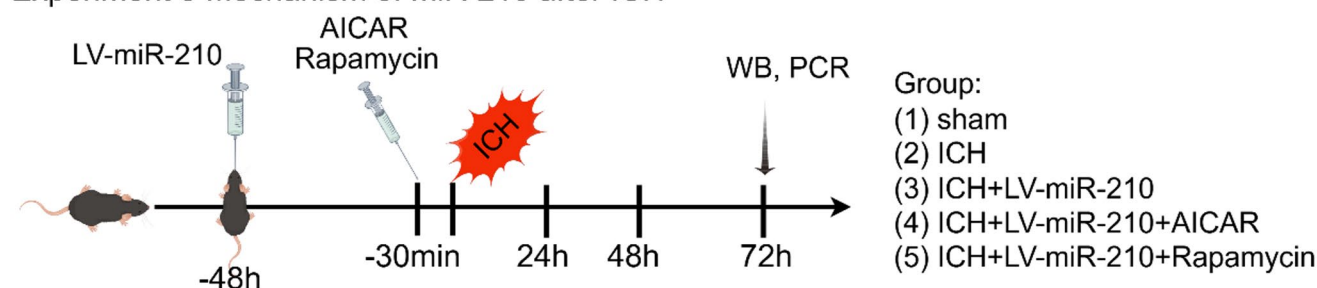


**Fig. 1.1** In Vivo experimental workflow and cohort stratification

administered intraperitoneally (IP) at a dose of 0.14 ml per 10 g of body weight. Under a stereoscopic microscope and using a microsyringe pump, 6  $\mu$ l of collagenase VII (Sigma–Aldrich, St. Louis, MO) were precisely infused into the left basal ganglia. The injection coordinates were set at 0.2 mm posterior to the coronal suture, 2.2 mm lateral to the sagittal suture, and 3.5 mm deep from the dura mater, in accordance with established guidelines [20]. Post-injection, the needle was kept in place for 5 min before being gently withdrawn, and the cranial hole was sealed with bone wax. For the sham control group, the needle insertion was performed without any collagenase injection.

### Injection of Drugs

*LV-miR-210-copGFP*, obtained from Youxi Weinan Biotechnology Co., Ltd. (located in Fujian, China), was utilized in this study. Precisely, 2.2  $\mu$ l of *LV-miR-210* solution containing a total titer of  $2 \times 10^9$  TU/ml, or an equivalent volume of saline, was infused into the lateral ventricle of the mice. The injection coordinates were established as 0.3 mm posterior to bregma, 1.0 mm lateral, and 2.3 mm deep, with the injection proceeding at a rate of 0.2 ml/min.

Furthermore, rapamycin and AICAR, both acquired from MedChemExpress (headquartered in Monmouth Junction, NJ, USA), were used in the experiment. The mice were injected with 2  $\mu$ l of 1  $\mu$ M/ml rapamycin and 2  $\mu$ l of 0.2  $\mu$ M/ml AICAR [21, 22], respectively, using the same injection technique as previously described.

The lentiviral concentration and time gradient experimental results, statistical trends of mNSS Score changes following surgery, and pharmacological safety and efficacy

evaluations post-administration are presented in Figure S1 and Supplementary file 1.

### Cell Culture and Experimental Design

HT22 cells were cultured in DMEM medium supplemented with 10% fetal bovine serum at 37 °C with 5% CO<sub>2</sub>, and the medium was changed every 48 h. The cells were treated with 200  $\mu$ M/L hemin [23] to establish an in vitro intracerebral hemorrhage model, which was divided into control group. The expression of miR-210 (gapdh normalized) was analyzed by qPCR in Hemin groups (3 h, 6 h, 12 h and 24 h), and 12 h was the best exposure time for subsequent intervention. Drug combination therapy studies combined LV-miR-210 with either AICAR (1.0 mmol/L, AMPK activator) or rapamycin (250 nmol/L, mTOR inhibitor) during hemin exposure [24], resulting in five groups: Sham group, ICH group, ICH+LV-miR-210 group, ICH+LV-miR-210+AICAR group and ICH+LV-miR-210+Rapamycin group. The protein levels of autophagy (LC3I/II, Beclin1), apoptosis (Bax, Bcl-2) and AMPK/mTOR signaling pathway (p-AMPK/AMPK, p-mTOR/mTOR) were analyzed by Western blot with  $\beta$ -actin as loading control. Cell grouping is shown in Fig. 1.2, Cell transfection and screening are detailed in Supplementary file 2.

### qPCR Analysis

RNA was extracted from brain tissue samples ( $n=6$  in each group, and 2 d after ICH induction in the sham group) using a total RNA extraction solution (Solarbio, Beijing, China; catalogue: R1100). RNA concentration was determined using a NanoDrop One spectrophotometer (Thermo, USA).

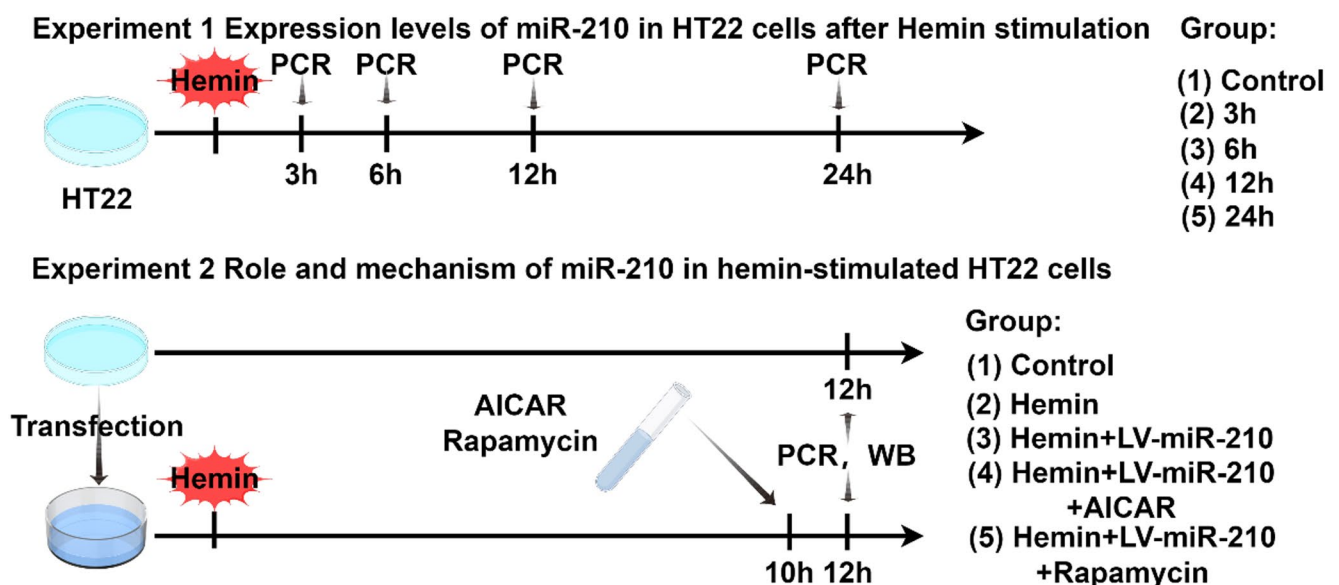


Fig. 1.2 In vitro experimental workflow and cohort stratification



The isolated RNA was then reverse transcribed into cDNA with PrimeScript™ RT Master Mix (TakaraBio, Japan; catalogue number: RR036A-1). qRT-PCR analysis was performed using BeyoFast™ SYBR Green qPCR Mix (2x, Low ROX) (Beyotime, Jiangsu, China; catalogue number: D7262) on a 7500 instrument (Thermo Fisher, USA). Target gene expression levels were normalized to GAPDH using a real-time fluorescent quantitative PCR system. The specific primers for qRT-PCR are listed in Table 1.

## Assessment of Neurological Deficits

Neurological deficits were assessed using the modified Neurological Severity Score (mNSS), a composite scale evaluating motor, sensory, cognitive, reflex, and abnormal movement functions, with scores ranging from 0 (normal) to 18 (maximal deficit) [25]. Higher scores indicate more severe neurological impairment. The mNSS was recorded for each experimental group at 7 d post-intracerebral hemorrhage (ICH) to quantify neurological dysfunction.

## Brain Edema Assessment

To measure brain water content, the standardized dry-wet technique was used. Following euthanasia, the mice brains were swiftly removed, and their wet weight was recorded. The brains were then dried at 100°C for 24 h to obtain the dry weight. Afterward, the percentage of brain water content was derived using the formula: [(wet weight minus dry weight) divided by wet tissue weight] multiplied by 100% [26].

## Western Blot Analysis

Tissue samples from the left hemisphere of mice were acquired for research purposes. Extraction of proteins was carried out using a tissue lysis buffer that incorporated

phosphatase inhibitors, protease inhibitors, and phenyl-methylsulfonyl fluoride to ensure thorough extraction of soluble proteins. A Thermo Fisher Scientific quinolinic acid kit facilitated the measurement of protein concentration. An equivalent quantity of protein was electrophoresed onto 10% SDS-PAGE gels. Post-electrophoresis, the proteins were transferred onto a PVDF membrane with a pore size of 0.45 µm for further analysis. A blocking procedure was performed using 5% non-fat milk for 2 h at 4 °C. Following this, the membranes were incubated overnight with specific antibodies directed against Bcl-2, Bax, LC3, Beclin 1, AMPK, p-AMPK, mTOR, p-mTOR, and β-actin, sourced from Proteintech Group (China) and Bioworld Technology (USA), among others, at a dilution of 1:800. Subsequently, the membranes were incubated with a secondary antibody, chosen based on the species and isotype of the primary antibody, for 2 h at 4°C with a dilution of 1:5000. Enhanced chemiluminescence was employed to visualize the immune signals.

## Immunofluorescence

After a 30-minute re-warming, the sections were washed three times with PBS containing 0.3% Triton X-100, each wash lasting 10 min. They were then blocked with 10% fetal bovine serum (FBS) for 1 h at 37°C. Subsequently, the sections were incubated overnight at 4°C with primary antibodies, such as anti-Iba-1 (Proteintech Group, USA; 10904-1-AP), anti-GFAP (Abcam, UK; ab278054), anti-NeuN (Abcam, UK; ab104224), and others, diluted 1:50. After three 5-minute PBS washes, the sections were treated with fluorescent secondary antibodies for 2 h at room temperature. Following three additional 5-minute PBS washes, they were stained with DAPI for 30 min. The sections were examined under a fluorescence microscope.

## TUNEL Staining

A TUNEL kit from Abbkine (catalogue number: KTA2010) was used to detect apoptosis in brain cells. Brain tissue sections were warmed to 37°C for 30 min and then fixed with 4% paraformaldehyde for 15 min. After two washes with PBS, the sections were treated with 20 µg/mL proteinase K at 37°C for 5 min. They were then washed with buffer for 5 min and incubated in a DNA labelling solution at 37°C for 1 h. After rinsing with PBS for 5 min, the sections were incubated in an antibody solution at 25°C for 30 min. Following a rinse with double-distilled water and an additional 5-minute incubation, the sections were mounted and sealed using DAPI Fluoromount-G.

**Table 1** Primer sequences utilized for qPCR analysis

Name	Sequence
MIR-210	F: AGCGTGCTGTGCGTGTGAC R: C AGTGCAGGGTCCGAGGTATT
GAPDH	F: GGCAAGTTCAACGGCACAGT R: ATGACATACTCAGCACCGGG
IL-1β	F: TCATTGTGGCTGTGGAGAAG R: AGGCCACAGGTATTTTGTCG
IL-6	F: GCCTTCTTGGGACTGATGCT R: TGGAAATTGGGGTAGGAAGGAC
IL-10	F: GCTCTTACTGACTGGCATGAG R: CGCAGCTCTAGGAGCATGTG
TNF-α	F: ACAGAAAGCATGATCCGCGA R: TTGCTACGACGTGGGCTAC
iNOS	F: CAAGAGTTTGACAGAGGACC R: TGGAACCACTCGTACTTGGGA

## Maze of Water

To evaluate cognitive functions (learning and memory) in mice, the Morris water maze test was conducted [22]. Training began the day after ICH. In each session, a mouse was placed in the center of one quadrant, facing the pool wall, and allowed to swim freely. Over five consecutive days, each mouse underwent four daily trials, followed immediately by placement in a dry cage after each trial. To ensure the recovery of strength and the maintenance of body temperature, the trials were performed 15 min. On day 7, the memory of each mouse was tested by placing the mouse in the quadrant farthest from the platform. ANY-maze, a path analysis software, was employed to assess latency, swimming speed, swimming distance, and additional parameters.

## Statistical Analysis

Data were expressed as mean  $\pm$  SEM. Comparisons of means among multiple groups were analyzed using one-way ANOVA. Image processing and data analysis were conducted using ImageJ software and GraphPad Prism (version 9.0). A  $P < 0.05$  was considered statistically significant.

## Results

### *miR-210* was Transiently and Significantly Upregulated in the Brain Tissue of Mice After ICH

qPCR analysis of brain tissue obtained from the ipsilateral (left) hemisphere of mice subjected to ICH has demonstrated (Fig. 2) that the overall expression of *miR-210* in brain tissue was upregulated following ICH, attaining a peak approximately 6 h post-injury, thereafter gradually declining. It is worth mentioning that the level of *miR-210* expression also rose in the opposite brain hemisphere.

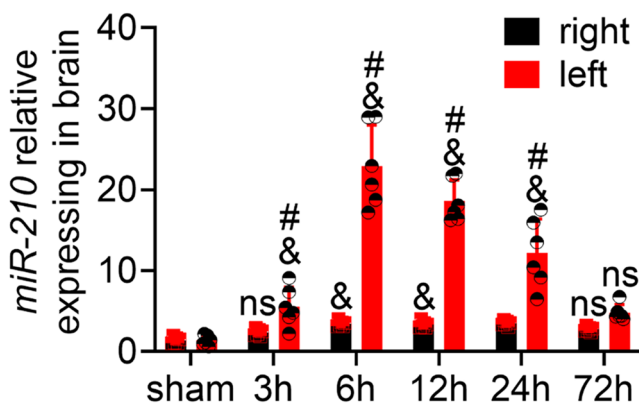


**Fig. 2** Levels of *miR-210* in mouse brain tissue post-intracerebral hemorrhage at various time points

However, this elevation was comparatively slower and less pronounced compared to that observed on the injured side.

Each experiment was repeated six times, and the findings are displayed as mean  $\pm$  SEM. The symbol # signifies  $P < 0.05$  when compared to the contralateral side, the notation & represents  $P < 0.05$  in relation to the sham group, ns mean  $P > 0.05$ .

### Achieving *miR-210* Overexpression in Mouse Brain via Lentiviral Vector Mediation

To ascertain the transfection efficacy of the lentiviral vector within the mouse brain, we conducted a study utilizing immunofluorescence dual staining to quantify the expression of the lentiviral vector in neuronal cells three days post-modeling (five days post-injection of the lentiviral vector into the lateral ventricle). The experimental findings demonstrated that copGFP was co-localized with NeuN, GFAP, and Iba-1, indicating that the lentiviral vector was capable of being expressed in neurons, astrocytes, and microglia (Fig. 3B). Furthermore, qPCR validation affirmed that *LV-miR-210* treatment led to a notable increase in *miR-210* expression in mouse brain tissue (Fig. 3C). Therefore, these findings suggested that *miR-210* could be effectively overexpressed in the mouse brain through gene transfection.

### In Mice, *miR-210* has the Potential to Mitigate Neurological Impairments and Decrease Cerebral Edema Following ICH

Following induced intracerebral hemorrhage (ICH), mice in the experimental groups showed notable cognitive and memory decline compared to the sham group. Specifically, the escape latency of mice in the ICH+LV group was substantially shorter than that of the ICH-only and ICH+NS groups (Fig. 4B). Additionally, the ICH+LV group spent less time searching for the target platform (Fig. 4C) and crossed it less frequently (Fig. 4D), indicating improved learning, cognitive function, and memory retention post-ICH with *miR-210* overexpression. The dry-wet method revealed that brain water content was lower in the *LV-miR-210*-treated ICH group compared to the ICH-only and ICH+NS groups (Fig. 4E). Furthermore, modified neurological severity scores (mNSSs) (Fig. 4F) showed that ICH compromised neurological function, but *LV-miR-210* treatment partially mitigated neurological dysfunction or facilitated recovery.

### *miR-210* Inhibited ICH-Induced Autophagy and Reduced Apoptosis and Neuroinflammation

As evidenced by the Western blotting analysis (Fig. 5A and B), both the ICH and ICH+NS groups displayed

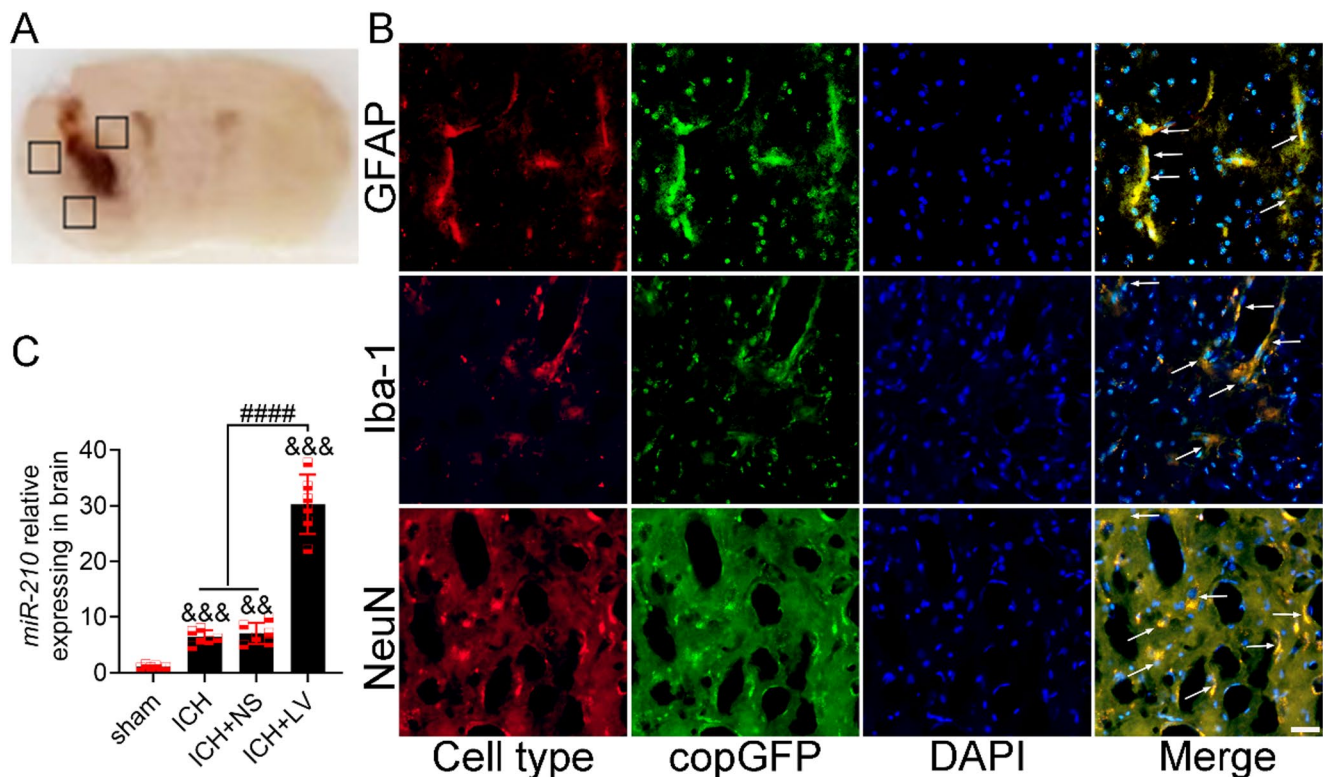


**Fig. 3** Lentivirus-mediated Expression of *miR-210* in Mouse Brain. **(A)** Coronal section of the mouse brain following induction of intracerebral hemorrhage (ICH); the designated boxes delineate the regions where immunofluorescence and TUNEL staining assessments were conducted. **(B)** Microscopic images demonstrating dual immunofluorescence staining for copGFP/NeuN, copGFP/GFAP, and copGFP/Iba-1 post lentiviral injection; scale bar equals 25 micrometers. **(C)**

PCR analysis was conducted five days post-administration of *LV-miR-210* and normal saline (NS) to quantify *miR-210* expression in ipsilateral brain tissue. Each experiment was replicated six times, and the results are presented as mean  $\pm$  SEM. #####Statistical significance:  $P < 0.0001$ ; &&& denotes  $P < 0.001$  when compared to the sham group; && denotes  $P < 0.01$  when compared to the sham group

significantly heightened protein expression of LC3-II, Beclin 1, and Bax compared to the sham group, while Bcl-2 levels were markedly decreased. In contrast, the *LV-miR-210-treated* group exhibited notably reduced protein levels of LC3-II, Beclin1, and Bax, along with a significant increase in Bcl-2 expression, compared to both the ICH and ICH+NS groups. The qPCR results further indicated that the mRNA levels of iNOS, IL-1 $\beta$ , IL-6, and TNF- $\alpha$  were substantially lower in the *LV-miR-210* group than in the ICH and ICH+NS groups, while the IL-10 mRNA level was comparatively higher (Fig. 5C). Additionally, the TUNEL assay results provided further verification (Fig. 5D and E) that *miR-210* overexpression alleviated ICH-induced apoptosis. Notably, *LV-miR-210* treatment resulted in decreased p-AMPK levels and increased p-mTOR levels (Fig. 5A and B). Taken together, these findings suggest that *miR-210* can suppress ICH-induced autophagy, reduce ICH-induced apoptosis and inflammation, and that this effect is partly mediated by modulation of the AMPK/mTOR signaling pathway.

### Activating the AMPK/mTOR Signaling Pathway Negated the Neuroprotective Benefits of *miR-210*

AICAR, the first discovered activator of AMPK, has been extensively utilized in research endeavors pertaining to AMPK. Animal experiments have shown that AICAR can activate AMPK in different tissues [27]. Western blot analysis revealed that *miR-210* inhibited ICH-induced AMPK phosphorylation (Fig. 5A and B), whereas the AMPK activator AICAR promoted AMPK phosphorylation (Fig. 6A and B) and, to some extent, inhibited mTOR phosphorylation. In addition, *miR-210* inhibited ICH-induced p-mTOR downregulation (Fig. 5A and B), and this impact was quenched by the mTOR inhibitor rapamycin (Fig. 6A and C). The results indicate that *miR-210* can inhibit the phosphorylation of components within the AMPK/mTOR signaling cascade.

AICAR and rapamycin abrogated the *miR-210*-mediated inhibition of Beclin1 and LC3II and upregulated these proteins (Fig. 6A and E, and 6H). Furthermore, the observed effect was an upregulation of Bax expression (refer to



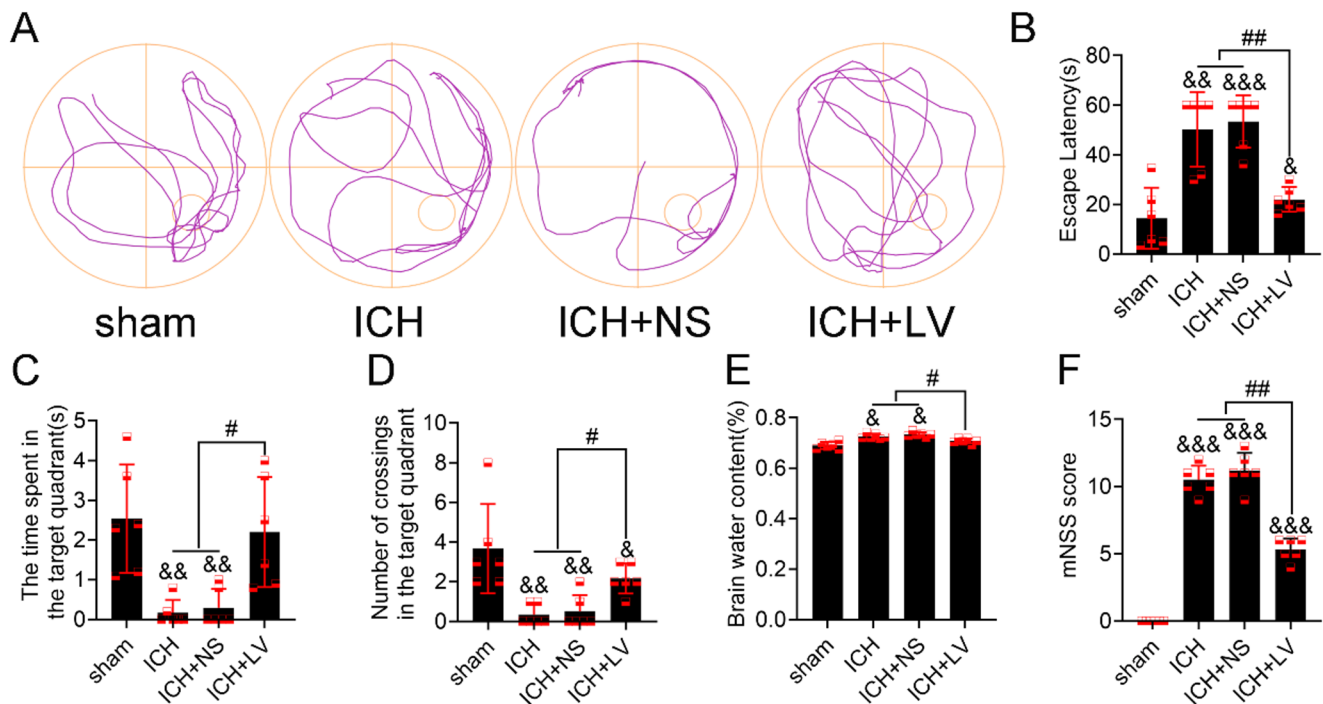


**Fig. 4** Depicts the impact of *miR-210* on neurological deficiencies and brain edema in mice following induced by ICH. **(A)** Typical swimming patterns of mice from each group were noted during the Morris water maze testing phase. **(B)** The study explored the effect of *miR-210* on the escape latency times observed in the Morris water maze test. **(C)** The instances of platform crossings encountered during the probe trial were documented. **(D)** The duration mice spent in the correct quadrant during the probe trial was measured. **(E)** Brain water content was individually measured for each group, albeit this information did not

directly correspond with the results of the probe trial. **(F)** Seven days post-ICH induction, modified neurological severity scores (mNSS) were assessed for mice in each group. All experiments were conducted six, yielding results presented as mean  $\pm$  SEM. Statistical significance:  $^{##}P<0.01$ ,  $^{*}P<0.05$  indicate significant differences compared to the sham group, with  $^{&&&}P<0.001$  and  $^{&&}P<0.01$  denoting highly significant and significant differences, respectively, when compared to the sham group's performance

Fig. 6A and F) and a corresponding downregulation of Bcl-2 expression (refer to Fig. 6A and G). Taken together, these findings indicate that promoting AMPK/mTOR phosphorylation partially reverses *miR-210*-mediated autophagy inhibition and protection against neuronal apoptosis.

### Role of *miR-210* in Hemin-Treated HT22 Cells

To further validate our results at the cellular level, we constructed an in vitro ICH model and conducted intervention experiments. Results As shown in Fig. 7A, after Hemin exposure (200  $\mu$ mol/L), the expression of *miR-210* in HT22 neurons was up-regulated in a time-dependent manner, reaching a peak at 6 h and 12 h, and then gradually decreasing, which established a time point for subsequent intervention. Lentiviral overexpression of *miR-210* synergistically amplified hemin-induced *miR-210* elevation (Fig. 7B), inhibited hemin-induced p-AMPK/AMPK activation and p-mTOR/mTOR inhibition, and resulted in decreased autophagy-related proteins LC3II/I and Beclin 1 and apoptosis-related protein Bax. While the increase of

Bcl-2 protein was increased, the use of AICAR and rapamycin significantly reversed the effect of *miR-210* (Fig. 7C and D).

### Discussion

The aim of this study was to investigate the effects of *miR-210* following intracerebral hemorrhage. Secondary brain injury mechanisms exhibit a partial overlap between intracerebral hemorrhage and cerebral ischemia, particularly in terms of inflammatory responses, oxidative stress, blood-brain barrier disruption, and apoptosis [3, 28]. Studies have indicated that *miR-210*'s expression and activity are crucial in brain cells, particularly in pathological scenarios such as brain tumors and ischemic brain damage. The transcription factor HIF-1 $\alpha$ , induced by hypoxia, regulates the expression of *miR-210-3p* in glioma cells. Increased *miR-210-3p* levels are linked to the advancement of epithelial-mesenchymal transition (EMT) and chemotherapy resistance, showing a strong connection with TGF- $\beta$  expression [29]. Furthermore, there are notable variations in *miR-210*

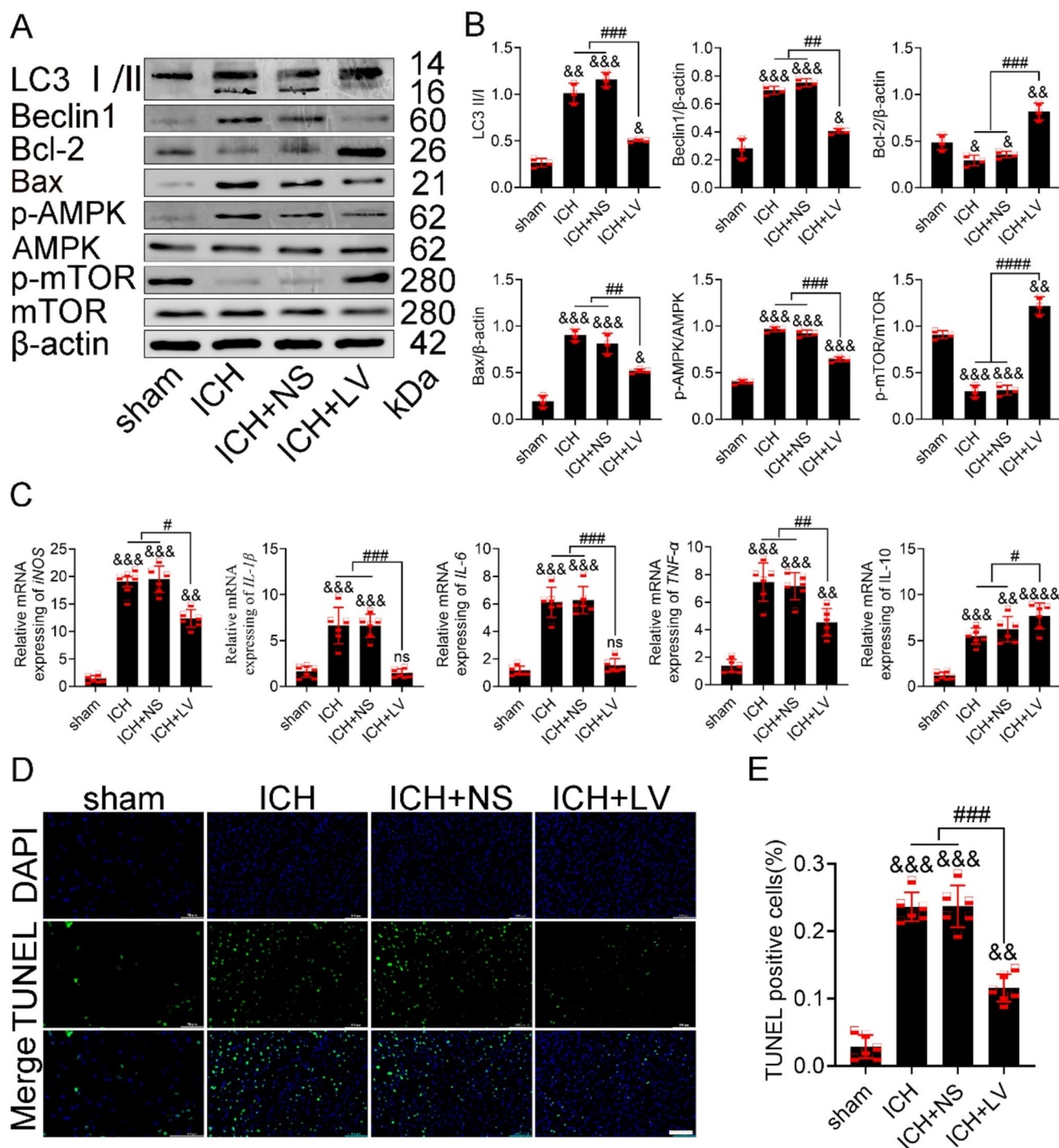


**Fig. 5** *miR-210* inhibited ICH-induced autophagy and attenuated apoptosis and neuroinflammation. **(A)** Western blot analysis was employed to measure Beclin1, Bax, and Bcl-2 levels, as well as the LC3II/I, p-AMPK/AMPK, and p-mTOR/mTOR ratios in the brain tissue of mice from each group. **(B)** A quantitative assessment was conducted to determine the protein levels of Beclin1, Bax, and Bcl-2, and the ratios of LC3II/I, p-AMPK/AMPK, and p-mTOR/mTOR. **(C)** Real-time PCR was used to investigate the expression of iNOS, IL-1β, IL-6, TNF-α, and IL-10 in the brain tissue of mice from each group.

**(D)** Brain sections were stained with TUNEL (green) to detect apoptotic cells and counterstained with DAPI (blue) to visualize nuclei; the scale bar is 100 μm. **(E)** The percentage of TUNEL-positive cells was calculated. All qPCR experiments were performed six times, WB experiments were performed three times, and the results are presented as mean ± SEM. Significance levels: #### $P < 0.0001$ , ### $P < 0.001$ , ## $P < 0.01$ , # $P < 0.05$ ; &&& $P < 0.001$ , && $P < 0.01$ , & $P < 0.05$  compared to the sham group

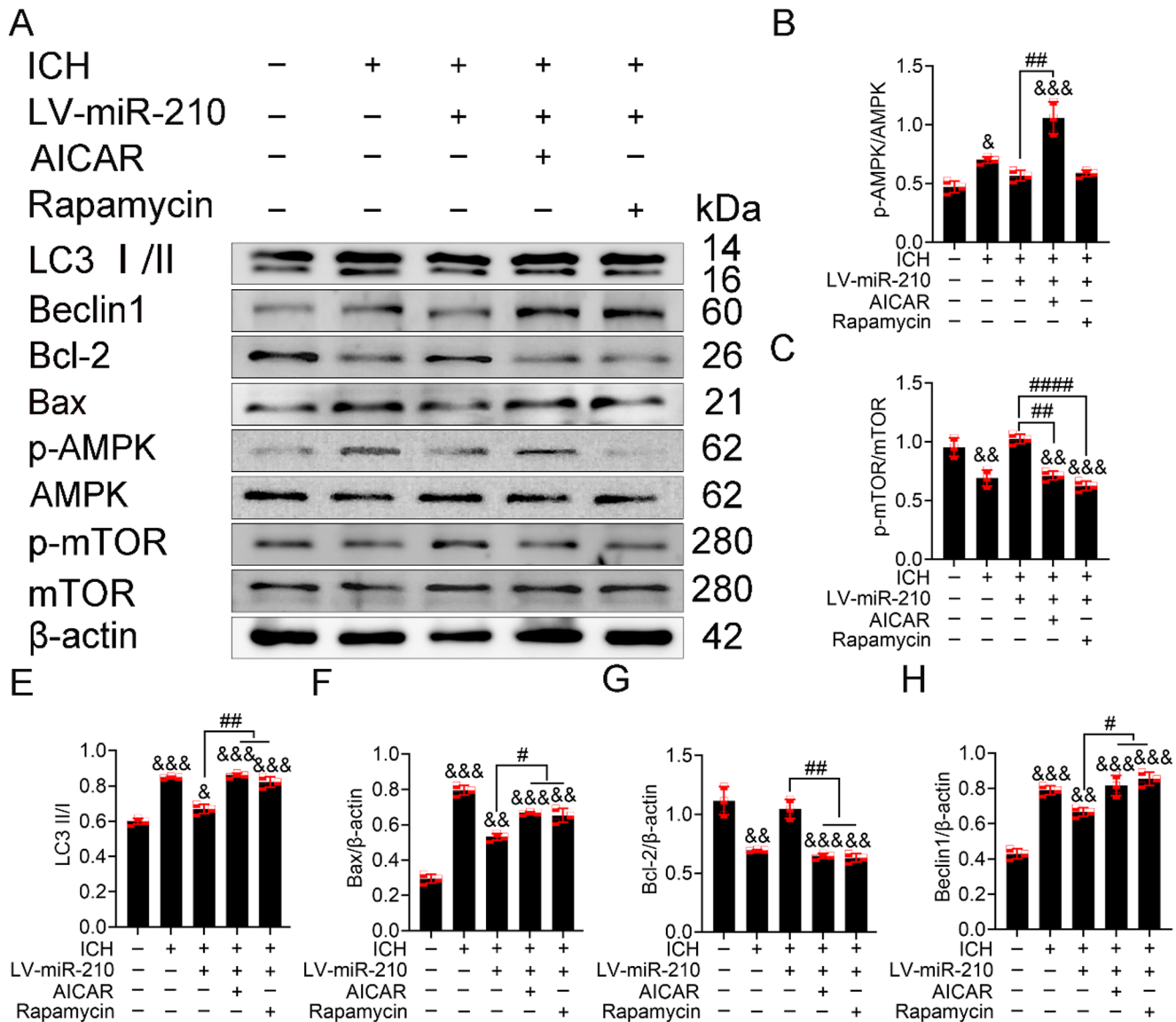


**Fig. 6** Promoted activation of AMPK/mTOR signaling reversed the neuroprotective effects of *miR-210*. (A) Western blot analysis was performed to assess the levels of Beclin 1, Bax, Bcl-2, and the ratios of LC3 II/I, p-AMPK/AMPK, and p-mTOR/mTOR in mouse brain tissue from each group. Subsequently, a quantitative evaluation was conducted specifically on the ratios of p-AMPK/AMPK, p-mTOR/

mTOR, and LC3II/I, as well as the protein abundance of Bax, Bcl-2, and Beclin1, as detailed in (B), (C), (D), (E), (F), (G), (H). All experiments were performed three times, and the results are presented as mean ± SEM. Significance levels: ##### $P < 0.0001$ , #### $P < 0.001$ , ## $P < 0.01$ , # $P < 0.05$ ; &&& $P < 0.001$ , && $P < 0.01$ , & $P < 0.05$  compared to the sham group

expression among patients with acute cerebral infarction, and its decreased expression is negatively correlated with patient survival rates, suggesting its potential value in the clinical diagnosis and prognosis of acute cerebral infarction [30]. *miR-210* also influences the migration of neural precursor cells (NPCs) under hypoxic conditions. Studies have indicated that bone marrow-derived mesenchymal stem cells (BMSCs) can enhance NPC migration under hypoxic conditions by upregulating *miR-210*, a process that may be linked to elevated VEGF-C levels [31]. This migratory ability is essential for nerve regeneration. Hence, the expression

level and role of *miR-210* in brain cells hold significance under various pathological circumstances.

This investigation has uncovered that *miR-210* offers significant protection against injury caused by ICH in mice. This protective effect is achieved by suppressing autophagy and apoptosis processes. Moreover, *miR-210* offers protection against subsequent damage after ICH, at least partially, by inhibiting autophagy regulated by the AMPK/ mTOR signaling pathway (Fig. 8). The levels of *miR-210* expression are tightly linked to the inflammatory response that follows ICH. Studies have shown that *miR-210* has the ability

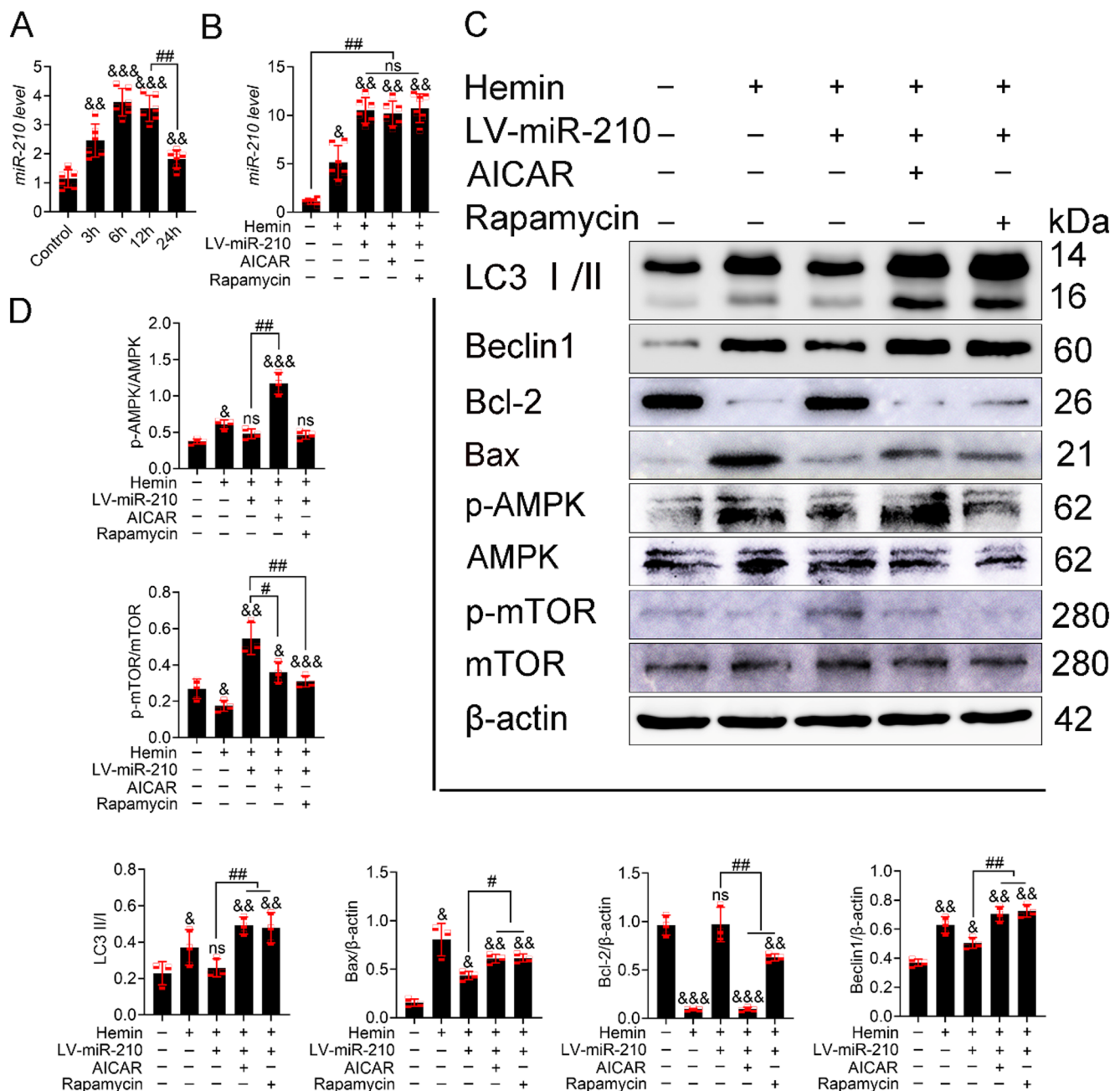


**Fig. 7** Role of miR-210 in Hemin-treated HT22 cells (**A**), (**B**) miR-210 level in each group; (**C**) Western blot analysis was performed to assess the levels of Beclin 1, Bax, Bcl-2, and the ratios of LC3 II/I, p-AMPK/AMPK, and p-mTOR/mTOR in HT22 from each group. Subsequently, a quantitative evaluation was conducted specifically on the ratios of p-AMPK/AMPK, p-mTOR/mTOR, and LC3II/I, as well as the pro-

tein abundance of Bax, Bcl-2, and Beclin1, as detailed in (**D**). All qPCR experiments were performed six times, WB experiments were performed three times, and the results are presented as mean  $\pm$  SEM. Significance levels: #####  $P < 0.0001$ , ###  $P < 0.001$ , ##  $P < 0.01$ , #  $P < 0.05$ ; &&&  $P < 0.001$ , &&  $P < 0.01$ , &  $P < 0.05$  compared to the sham group

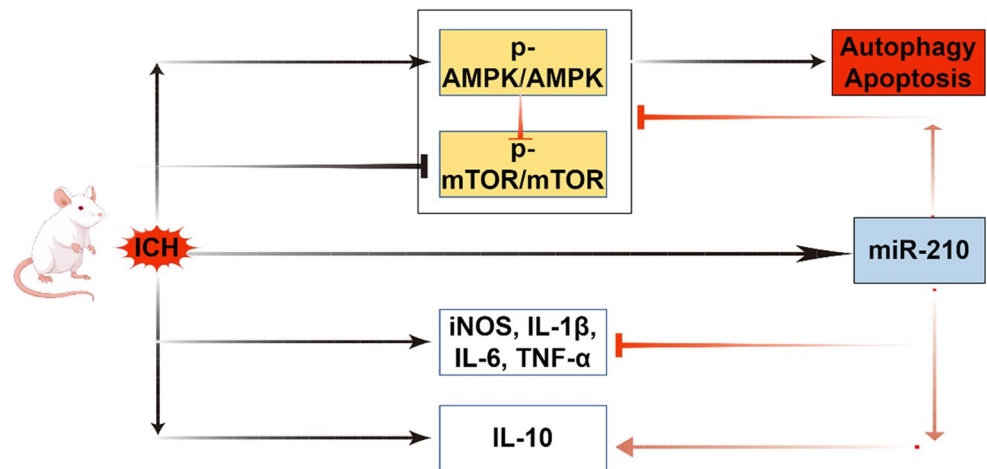
to downregulate the expression of pro-inflammatory factors, consequently alleviating the inflammatory harm to brain tissue. This suppression may contribute to reducing secondary brain injury and enhancing neurological function recovery. In this study, the administration of *miR-210* resulted in improved motor function and decreased brain swelling,

which further confirms its neuroprotective role following ICH.

*miR-210* has emerged as a potential biomarker, with variations in its expression levels linked to patient functional recovery and long-term survival [30]. These observations imply that *miR-210* could serve both as a diagnostic marker and a significant predictor of treatment response [30, 32].



**Fig. 8** miR-210 regulates autophagy and apoptosis through AMPK/mTOR



While *miR-210*'s dysregulation in both ICH and ischemic stroke limits its specificity as a stand-alone diagnostic biomarker, its temporal expression kinetics (e.g., acute-phase elevation in ICH vs. subacute decline in ischemia) may complement imaging modalities. For instance, *miR-210* quantification in ambulances or imaging-limited settings could prioritize patients requiring urgent neuroprotection prior to definitive CT/MRI diagnosis. Our research has demonstrated a significant upregulation of *miR-210* expression in cerebral tissue following ICH in mice, highlighting its neuroprotective role. This suggests that *miR-210* may represent a promising therapeutic target for reducing secondary injuries after ICH. We are optimistic that continued and forthcoming research will further promote its clinical application.

This study has several limitations. Due to concerns regarding hormonal fluctuations potentially confounding experimental stability in female mice, coupled with epidemiological evidence indicating higher susceptibility to intracerebral hemorrhage (ICH) in males [33], we exclusively utilized male subjects in our preclinical model. However, this sex-specific design inevitably restricts the generalizability of our findings to female populations. Future clinical validations will incorporate mixed-sex cohorts to enhance translational relevance. Notably, while our PCR and western blot analyses focused on basal ganglia-derived homogenates (the primary hematoma site in our collagenase-induced model), this spatially restricted sampling strategy, though ensuring standardized intergroup comparisons aligned with systemic therapeutic targeting, precluded detection of region-specific *miR-210* expression dynamics. In addition, circulating *miR-210* has been identified as a diagnostic biomarker with reduced expression in ischemic stroke patients [34], our data paradoxically demonstrate *miR-210* upregulation in murine ICH models. This divergence suggests *miR-210* may serve as a differential diagnostic marker between hemorrhagic and ischemic stroke subtypes; however, the

absence of clinical ICH validation cohorts weakens this hypothesis.

Furthermore, the neuroprotective role of *miR-210* in ICH—potentially mediated through autophagy modulation, anti-apoptotic effects, or inflammatory suppression—requires mechanistic validation. Importantly, the contrasting expression patterns between ischemic and hemorrhagic stroke subtypes raise concerns about therapeutic targeting: *miR-210* agonism in ICH may inadvertently exacerbate ischemic vulnerability. Future studies will rigorously evaluate the context-dependent efficacy and safety profiles of *miR-210* manipulation, utilizing cell-type-specific knockout models and dual pathology assessments.

## Conclusions

In summary, *miR-210* has a neuroprotective effect in vivo after ICH and can inhibit autophagy, apoptosis and neuroinflammation induced by ICH to a certain extent, at least in part through the AMPK/mTOR signalling pathway. *miR-210* could be a promising candidate for preventing and treating secondary injury in haemorrhagic stroke patients.

**Supplementary Information** The online version contains supplementary material available at <https://doi.org/10.1007/s11064-025-04434-7>.

**Acknowledgements** None.

**Author Contributions** Y.W., L. J. and J.T. took charge of executing the experiments and analyzing the data. L.Z., H.D., C.G., L.Z., L.W., Y.L. and Y.Z. all contributed to drafting the paper. All authors have reviewed and given their approval to the manuscript's final version.

**Funding** The work was supported by Postgraduate Research & Practice Innovation Program of Jiangsu Province (SJCX24\_2069), the General program of clinical basic Research in Nantong University (2022JY003), The first phase of "Research Innovation Team Project" of Kangda College of Nanjing Medical University (KD2022KY-

CXTD006), National Key Laboratory of Oncology System Medicine Open Fund (KF2203-93), National Natural Science Foundation of China (82074524), Project of Nantong Health Commission (MS2023073, MS2022014), Clinical Research Program of Nantong University (2022LY009), Nursing Research Program of Nantong University (2022HY003), Jiangsu Traditional Chinese Medicine Science and Technology Development Program Project (MS2021060), Nantong science and technology project (MSZ2023156), Research Project of Kangda College, Nanjing Medical University (KD-2023KYJJ269), Nantong university 2023 clinical medicine special project (2023HY001), Guiding Project of Health Commission of Jiangsu Province (Z2022067), Educational Research Project of Kanda College of Nanjing Medical University (KD2022JYYJZD005).

**Data Availability** No datasets were generated or analysed during the current study.

## Declarations

**Ethics Approval and Consent to Participate** The protocol for animal experimentation was approved by the Ethics Committee of the Nantong University Laboratory Animal Center. The study results are reported adhering to ARRIVE guidelines, and the protocol number is (S20220221-035).

**Consent for Publication** Not applicable.

**Competing Interests** The authors declare no competing interests.

**Open Access** This article is licensed under a Creative Commons Attribution-NonCommercial-NoDerivatives 4.0 International License, which permits any non-commercial use, sharing, distribution and reproduction in any medium or format, as long as you give appropriate credit to the original author(s) and the source, provide a link to the Creative Commons licence, and indicate if you modified the licensed material. You do not have permission under this licence to share adapted material derived from this article or parts of it. The images or other third party material in this article are included in the article's Creative Commons licence, unless indicated otherwise in a credit line to the material. If material is not included in the article's Creative Commons licence and your intended use is not permitted by statutory regulation or exceeds the permitted use, you will need to obtain permission directly from the copyright holder. To view a copy of this licence, visit <http://creativecommons.org/licenses/by-nc-nd/4.0/>.

## References

- Li X, Feng D, Chen G (2018) An update on medical treatment for intracerebral hemorrhage. *Transl Stroke Res* Published Online September 11. <https://doi.org/10.1007/s12975-018-0664-5>
- Verhoeven JI, Pasi M, Casolla B et al (2021) Long-term mortality in young patients with spontaneous intracerebral haemorrhage: predictors and causes of death. *Eur Stroke J* 6(2):185–193. <https://doi.org/10.1177/23969873211017723>
- Magid-Bernstein J, Girard R, Polster S, Srinath A, Romanos S, Awad IA, Sansing LH (2022) Cerebral hemorrhage: pathophysiology, treatment, and future directions. *Circ Res* 130(8):1204–1229. <https://doi.org/10.1161/CIRCRESAHA.121.319949Epub> 2022 Apr 14. PMID: 35420918; PMCID: PMC10032582
- Zhao L, Chen S, Sherchan P et al (2018) Recombinant CTRP9 administration attenuates neuroinflammation via activating adiponectin receptor 1 after intracerebral hemorrhage in mice. *J Neuroinflammation* 15(1):215. <https://doi.org/10.1186/s12974-018-1256-8>. Published 2018 Jul 30
- Zhou Y, Wang Y, Wang J, Anne Stetler R, Yang QW (2014) Inflammation in intracerebral hemorrhage: from mechanisms to clinical translation. *Prog Neurobiol* 115:25–44. <https://doi.org/10.1016/j.pneurobio.2013.11.003>
- Chen S, Zhao L, Sherchan P et al (2018) Activation of melanocortin receptor 4 with RO27-3225 attenuates neuroinflammation through AMPK/JNK/p38 MAPK pathway after intracerebral hemorrhage in mice. *J Neuroinflammation* 15(1):106. <https://doi.org/10.1186/s12974-018-1140-6>. Published 2018 Apr 11
- Ko JY, Lian WS, Tsai TC et al (2019) MicroRNA-29a mitigates subacromial Bursa fibrosis in rotator cuff lesion with shoulder stiffness. *Int J Mol Sci* 20(22):5742 Published 2019 Nov 15. <http://doi.org/10.3390/ijms20225742>
- Wang X, Xu H, Wang Y, Shen C, Ma L, Zhao C (2020) MicroRNA-124a contributes to glucocorticoid resistance in acute-on-chronic liver failure by negatively regulating glucocorticoid receptor alpha. *Ann Hepatol* 19(2):214–221. <https://doi.org/10.1016/j.aohep.2019.08.007>
- Melichar B, Plebani M (2011) Laboratory medicine: an essential partner in the care of cancer patients. *Clin Chem Lab Med* 49(10):1575–1578. <https://doi.org/10.1515/CCLM.2011.244>
- Li B, Dasgupta C, Huang L, Meng X, Zhang L (2020) MiRNA-210 induces microglial activation and regulates microglia-mediated neuroinflammation in neonatal hypoxic-ischemic encephalopathy. *Cell Mol Immunol* 17(9):976–991. <https://doi.org/10.1038/s41423-019-0257-6>
- Devlin C, Greco S, Martelli F, Ivan M (2011) miR-210: more than a silent player in hypoxia. *IUBMB Life* 63(2):94–100. <https://doi.org/10.1002/iub.427>
- Nollet E, Hoymans VY, Van Craenenbroeck AH, Vrints CJ, Van Craenenbroeck EM (2016) Improving stem cell therapy in cardiovascular diseases: the potential role of MicroRNA. *Am J Physiol Heart Circ Physiol* 311(1):H207–H218. <https://doi.org/10.1152/ajpheart.00239.2016>
- Wang H, Flach H, Onizawa M, Wei L, McManus MT, Weiss A (2014) Negative regulation of Hif1a expression and TH17 differentiation by the hypoxia-regulated MicroRNA miR-210. *Nat Immunol* 15(4):393–401. <https://doi.org/10.1038/ni.2846>
- Fan X, Zhang Y, Dong H, Wang B, Ji H, Liu X (2015) Trilobatin attenuates the LPS-mediated inflammatory response by suppressing the NF- $\kappa$ B signaling pathway. *Food Chem* 166:609–615. <https://doi.org/10.1016/j.foodchem.2014.06.022>
- Haseeb A, Khan NM, Ashruf OS, Haqqi TM (2017) A Polyphenol-rich pomegranate fruit extract suppresses NF- $\kappa$ B and IL-6 expression by blocking the activation of IKK $\beta$  and NIK in primary human chondrocytes. *Phytother Res* 31(5):778–782. <https://doi.org/10.1002/ptr.5799Epub> 2017 Mar 9. PMID: 28276100; PMCID: PMC5548175
- Bi S, Zhang Y, Zhou J et al (2023) miR-210 promotes hepatocellular carcinoma progression by modulating macrophage autophagy through PI3K/AKT/mTOR signaling. *Biochem Biophys Res Commun* 662:47–57. <https://doi.org/10.1016/j.bbrc.2023.04.055>
- Song R, Dasgupta C, Mulder C, Zhang L (2022) MicroRNA-210 controls mitochondrial metabolism and protects heart function in myocardial infarction. *Circulation* 145(15):1140–1153. <https://doi.org/10.1161/CIRCULATIONAHA.121.056929>
- Wang CS, Zhang XB, Zhu XT, Chen RS (2022) NBR2/miR-561-5p/DLC1 axis inhibited the development of multiple myeloma by activating the AMPK/mTOR pathway to repress Glycolysis. *Neoplasia* 69(5):1165–1174. [https://doi.org/10.4149/neo\\_2022\\_211102N1559](https://doi.org/10.4149/neo_2022_211102N1559)
- Tana C, Giamberardino MA, Cipollone F (2017) MicroRNA profiling in atherosclerosis, diabetes, and migraine. *Ann Med* 49(2):93–105. <https://doi.org/10.1080/07853890.2016.1226515>

20. Chen S, Peng J, Sherchan P et al (2020) TREM2 activation attenuates neuroinflammation and neuronal apoptosis via PI3K/Akt pathway after intracerebral hemorrhage in mice. *J Neuroinflammation* 17(1):168. <https://doi.org/10.1186/s12974-020-01853-x>. Published 2020 May 28
21. Sales AJ, Fogaça MV, Sartim AG, Pereira VS, Wegener G, Guimarães FS, Joca SRL (2019) Cannabidiol Induces Rapid and Sustained Antidepressant-Like Effects Through Increased BDNF Signaling and Synaptogenesis in the Prefrontal Cortex. *Mol Neurobiol.*;56(2):1070–1081. <https://doi.org/10.1007/s12035-018-1143-4>. Epub 2018 Jun 4. PMID: 29869197
22. Tanida M, Yamamoto N (2011) Central AMP-activated protein kinase affects sympathetic nerve activity in rats. *Neurosci Lett* 503(3):167–170. <https://doi.org/10.1016/j.neulet.2011.08.013> Epub 2011 Aug 27. PMID: 21893163
23. Cao Y, Li Y, He C, Yan F, Li JR, Xu HZ, Zhuang JF, Zhou H, Peng YC, Fu XJ, Lu XY, Yao Y, Wei YY, Tong Y, Zhou YF, Wang L (2021) Selective ferroptosis inhibitor Liproxstatin-1 attenuates neurological deficits and neuroinflammation after subarachnoid hemorrhage. *Neurosci Bull* 37(4):535–549 Epub 2021 Jan 9. PMID: 33421025; PMCID: PMC8055759
24. Zhang Y, Liu L, Hou X, Zhang Z, Zhou X, Gao W (2023) Role of autophagy mediated by AMPK/DDIT4/mTOR Axis in HT22 cells under oxygen and glucose deprivation/reoxygenation. *ACS Omega* 8(10):9221–9229. <https://doi.org/10.1021/acsomega.2c07280> PMID: 36936290; PMCID: PMC10018509
25. Hua Y, Schallert T, Keep RF, Wu J, Hoff JT, Xi G (2002) Behavioral tests after intracerebral hemorrhage in the rat. *Stroke.*;33(10):2478–84. <https://doi.org/10.1161/01.str.0000032302.91894.0f>. PMID: 12364741
26. Yin C, Huang GF, Sun XC, Guo Z, Zhang JH (2017) DLK Silencing attenuated neuron apoptosis through JIP3/MA2K7/JNK pathway in early brain injury after SAH in rats. *Neurobiol Dis* 103:133–143. <https://doi.org/10.1016/j.nbd.2017.04.006>
27. Li Y, Chen Y (2019) AMPK and autophagy. *Adv Exp Med Biol* 1206:85–108. [https://doi.org/10.1007/978-981-15-0602-4\\_4](https://doi.org/10.1007/978-981-15-0602-4_4)
28. Zhao Y, Zhang X, Chen X, Wei Y (2022) Neuronal injuries in cerebral infarction and ischemic stroke: from mechanisms to treatment (Review). *Int J Mol Med* 49(2):15. <https://doi.org/10.3892/ijmm.2021.5070>
29. Liu H, Chen C, Zeng J, Zhao Z, Hu Q (2021) MicroRNA-210-3p is transcriptionally upregulated by hypoxia induction and thus promoting EMT and chemoresistance in glioma cells. *PLoS ONE* 16(7):e0253522 Published 2021 Jul 1. <https://doi.org/10.1371/journal.pone.0253522>
30. Aderinto N, Olatunji G, Kokori E, Sanker V, Yusuf IA, Adefusi TO, Egbunu E, Aboje JE, Apampa OO, Ogieuhi IJ, Obasanjo OM, Awuah WA (2024) miR-210 in ischaemic stroke: biomarker potential, challenges and future perspectives. *Eur J Med Res* 29(1):432. <https://doi.org/10.1186/s40001-024-02029-6>
31. Wang F, Zhu J, Zheng J, Duan W, Zhou Z (2020) miR-210 enhances mesenchymal stem cellmodulated neural precursor cell migration. *Mol Med Rep* 21(6):2405–2414. <https://doi.org/10.3892/mmr.2020.11065>
32. Jin Y, Xiao P, Lai B, Huang L, Luo Q, Chen X (2023) Highly expressed miR-210 in the peripheral blood is closely associated with asphyxiated neonates. *Transl Pediatr* 12(6):1181–1191. <https://doi.org/10.21037/tp-23-106>
33. Appelros P, Stegmayr B, Terént A. Sex differences in stroke epidemiology: a systematic review. *Stroke*. 2009;40(4):1082–90. doi: 10.1161/STROKEAHA.108.540781. Epub 2009 Feb 10. PMID: 19211488.
34. Rahmati M, Ferns GA, Mobarra N. The lower expression of circulating miR-210 and elevated serum levels of HIF-1 $\alpha$  in ischemic stroke; Possible markers for diagnosis and disease prediction. *J Clin Lab Anal*. 2021;35(12):e24073. doi: 10.1002/jcla.24073.

**Publisher's Note** Springer Nature remains neutral with regard to jurisdictional claims in published maps and institutional affiliations.